Spin-susceptibility and spin-density excitations of the quasi-one-dimensional interacting electron gas: many-body effects for cylindrical confinement

1998 J. Phys.: Condens. Matter 10 4625

(http://iopscience.iop.org/0953-8984/10/21/018)

J. Phys.: Condens. Matter **10** (1998) 4625–4636. Printed in the UK PII: S0953-8984(98)91644-7

Spin-susceptibility and spin-density excitations of the quasi-one-dimensional interacting electron gas: many-body effects for cylindrical confinement

A Gold† and L Calmels‡

† Centre d'Elaboration de Matériaux et d'Etudes Structurales (CEMES–CNRS), 29 Rue Jeanne Marvig, 31055 Toulouse, France

‡ Department of Physics and Astronomy, University of Wales, Cardiff CF2 3YB, UK

Received 13 February 1998

Abstract. We calculate the ground-state energy of a quasi-one-dimensional electron gas with Coulomb interaction depending on the spin-polarization parameter ξ and the Wigner–Seitz parameter r_s. Cylindrical quantum wires of radius R_0 are considered. We describe the pair-correlation function $g(z = 0)$ as a function of r_s and ξ. We derive the spin-susceptibility as a function of R_0 and r_s in different approximations. Numerical results obtained for the spin-susceptibility are fitted by an analytical expression. Collective modes (charge-density and spin-density excitations) in cylindrical quantum wires are described and the validity range of our calculation is discussed.

1. Introduction

In two recent papers we have calculated the density dependence of the ground-state energy and the compressibility [1] and the spin-polarization dependence of the ground-state energy and the spin-susceptibility [2] of the quasi-one-dimensional electron gas with a *parabolic* confinement potential. The long-range Coulomb interaction of the electrons is taken into account. We used the sum-rule version of the Singwi–Tosi–Land–Sjölander (STLS) [3] approach. The STLS approach is a very useful approach to describe many-body effects in the low-density regime of interacting quantum systems [4] where the random-phase approximation (RPA) [5] fails to give quantitative results. The modification of the RPA with a local-field correction (LFC), for instance via the STLS approach, improves the validity range considerably. To calculate the spin-susceptibility we generalized the STLS approach in order to describe spin-polarization effects [2].

In the present paper we describe in more detail some aspects of our calculation and we study a *cylindrical* confinement potential. We discuss the validity range of our approach in detail. This is of importance because for long-range interaction potentials exact results are not available. We use a cylindrical confinement potential where the wire width is described by its radius R_0. In that case the Fourier transform of the interaction potential is given in analytical form [6]. Many-body effects for the unpolarized electron gas have been already described for this model within the STLS approach [7].

The paper is organized as follows. In section 2 we introduce the model. The theory is briefly described in section 3. The results of our calculation (spin-susceptibility and spin-density excitations) are given in section 4. The discussion of our results (validity range and experiments) is presented in section 5. We conclude in section 6.

0953-8984/98/214625+12$19.50

2. Model

For an electron gas in one dimension the Wigner–Seitz parameter r_s is given by the one-dimensional electron density N as $r_s = 1/2Na^*$. $a^* = \varepsilon_L/m^*e^2$ is the effective Bohr radius defined with the effective electron mass m^*, the background dielectric constant ε_L and the electron charge e. The energy scale is given by the effective Rydberg $\mathrm{Ry}^* = 1/2m^*a^{*2}$ with the Planck constant $h/2\pi = 1$. The electron density defines the Fermi wavenumber k_F via $N = 2k_F/\pi$. The spin-polarization parameter ξ with $0 \leqslant \xi \leqslant 1$ is expressed as $\xi = (N_+ - N_-)/N$ with $N = N_+ + N_-$ and the electron densities $N_\pm$ are given by $N_\pm = N(1 \pm \xi)/2$. The Fermi wavenumbers of the polarized subsystems are written as $k_{F\pm} = k_F(1 \pm \xi) = \pi N_\pm$. We assume that only the lowest one-dimensional subband is occupied (one-subband model) and our calculation is made for zero temperature.

The Fourier transform of the interaction potential is written as $V(q, \lambda) = \lambda V(q)$ where $0 \leqslant \lambda \leqslant 1$ is the coupling constant. We assume a cylindrical confinement in the xy-plane with R_0 as the wire radius and electrons are free to move in the z-direction. The Coulomb interaction potential $V(q)$ in the Fourier space is expressed as [6]

$$V(q) = \frac{e^2}{2\varepsilon_L} f(qR_0) \tag{1a}$$

with

$$f(x) = \frac{144}{x^2}\left[\frac{1}{10} - \frac{2}{3x^2} + \frac{32}{3x^4} - 64\frac{I_3(|x|)K_3(|x|)}{x^4}\right]. \tag{1b}$$

$I_3(x)$ and $K_3(x)$ are Bessel functions. The one-subband model implies that the Fermi energy $\varepsilon_F/\mathrm{Ry}^* = (k_F a^*)^2$ must be smaller than the intersubband energy $\Delta E_{12}/\mathrm{Ry}^* \approx 9a^{*2}/R_0^2$ [6] which leads to $r_s > r_s^* \approx R_0/4a^*$ for the unpolarized system. For $r_s < r_s^*$ at least two subbands are occupied.

3. Theory

The ground-state energy per particle $\varepsilon_0(r_s, \xi)$ of the polarized electron gas is given in terms of the kinetic, the exchange and the correlation contributions as $\varepsilon_0(r_s, \xi) = \varepsilon_{kin}(r_s, \xi) + \varepsilon_{ex}(r_s, \xi) + \varepsilon_{cor}(r_s, \xi)$. For the one-dimensional electron gas the kinetic energy per particle is given by $\varepsilon_{kin}(r_s, \xi)/\mathrm{Ry}^* = \pi^2(1 + 3\xi^2)/48r_s^2$. The Hartree energy is zero: we consider a model where a positive jellium gives rise to a *local* neutrality. The interaction energy is expressed by the exchange and the correlation contributions as $\varepsilon_{int}(r_s, \xi) = \varepsilon_{ex}(r_s, \xi) + \varepsilon_{cor}(r_s, \xi)$ and is written as

$$\varepsilon_{int}(r_s, \xi)/\mathrm{Ry}^* = \frac{a^*}{2\pi}\int_0^\infty \mathrm{d}q\, f(qR_0)\int_0^1 \mathrm{d}\lambda\,[S(q, \xi, \lambda) - 1]. \tag{2}$$

We use a generalized Feynman–Bijl expression for the static structure factor (SSF) $S(q, \xi, \lambda)$, which is given in terms of the contributions of the electron–hole excitations and the collective modes. For the SSF of the spin-polarized electron gas we obtain the analytical result [2]

$$S(q, \xi, \lambda) = 1/[1/S_0(q, \xi)^2 + \lambda/S_p(q, \xi, \lambda)^2]^{1/2}. \tag{3}$$

$S_0(q, \xi)$ is the SSF of the free polarized electron gas (particle–hole excitations) and the second term gives the contribution of the plasmon excitations due to the Coulomb interaction. $S_0(q, \xi)$ is given by $S_0(q, \xi) = (1 + \xi)S_{0+}(q)/2 + (1 - \xi)S_{0-}(q)/2$ with $S_{0\pm}(q \leqslant 2k_{F\pm}) = |q|/2k_{F\pm}$ and $S_{0\pm}(q \geqslant 2k_{F\pm}) = 1$. The term $S_p(q, \xi, \lambda)$ is given by

$S_p(q,\xi,\lambda) = [q^2/4m^*NV(q)[1 - G(q,\xi,\lambda)]]^{1/2}$ where the spin-polarization only enters via the LFC $G(q,\xi,\lambda)$.

By neglecting $G(q,\xi,\lambda)$ in the SSF, we obtain the mean-spherical approximation (MSA) [8], which is very similar to the RPA. Note, however, that within the RPA $S(q,\xi=0)$ is calculated numerically as a frequency integral over the dynamical SSF. Within the MSA the analytical form of the SSF as given in equation (3) is used. The Hartree–Fock approximation (HFA) for the ground-state energy is obtained by using the SSF of the free electron gas $S_0(q,\xi)$ in equation (2). In the HFA only exchange effects are taken into account and correlation effects are neglected. For the LFC we use the three-sum-rule approach of the STLS theory, where the LFC is described by

$$G(q,\xi,\lambda) = r_s \frac{a^*}{\pi R_0 C_2} \frac{f([q^2R_0^2 - |q|q_0R_0^2C_3 + q_0^2R_0^2/C_1^2]^{1/2})}{f(qR_0)}. \tag{4}$$

The coefficients $C_1 = C_1(r_s, R_0, \xi, \lambda)$, $C_2 = C_2(r_s, R_0, \xi, \lambda)$ and $C_3 = C_3(r_s, R_0, \xi, \lambda)$ are determined self-consistently [1]. The wavenumber q_0 is given by $q_0 = 2/r_s^{1/2}a^*$.

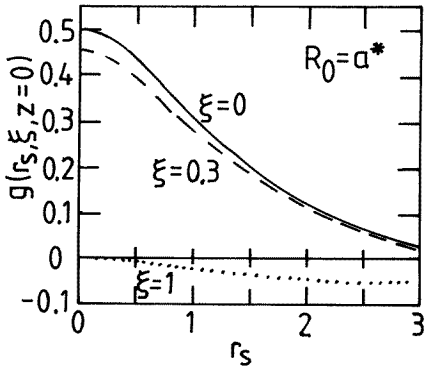

Figure 1. Pair-correlation function $g(r_s,\xi,z=0)$ versus Wigner–Seitz parameter r_s for different values of the spin-polarization parameter ξ and for wire width $R_0 = a^*$.

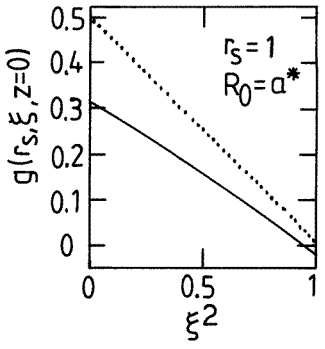

Figure 2. Pair-correlation function $g(r_s,\xi,z=0)$ versus spin-polarization parameter ξ^2 for $r_s = 1$ and $R_0 = a^*$. The dotted line represents the HFA.

The pair-correlation function $g(r_s,\xi,z)$ is obtained from the SSF by a Fourier transform [5], which gives, for $z = 0$, the analytical result [3]

$$g(r_s,\xi,z=0) = 1 - G(q\to\infty,\xi,\lambda=1). \tag{5a}$$

With the HFA for the LFC one obtains $G_{HFA}(q\to\infty,\xi,\lambda=1) = (1+\xi^2)/2$ and we find

$$g_{HFA}(r_s,\xi,z=0) = (1-\xi^2)/2. \tag{5b}$$

In figure 1 we show $g(r_s, \xi, z = 0)$ versus r_s and in figure 2 we show $g(r_s, \xi, z = 0)$ versus ξ^2. Even for large r_s, $g(r_s, \xi = 1, z = 0)$ is only slightly negative. The fact that the pair-correlation function $g(r_s, \xi = 0, z = 0)$ becomes negative at large r_s is a well known defect of the STLS approach [4]. The results obtained for the pair-correlation function show that our approach gives reasonable values. This is not a trivial point because the STLS approach is not exact. Moreover we use a three-sum-rule approach for the LFC together with an analytical expression for the SSF. These two additional approximations simplify the numerical calculations considerably.

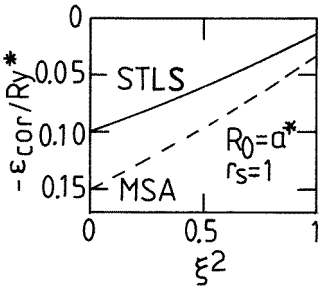

Figure 3. Correlation energy ε_{cor} versus spin-polarization parameter ξ^2 for $r_s = 1$ and $R_0 = a^*$. The solid line represents the STLS approach and the dashed line the MSA.

Our results for the correlation energy $\varepsilon_{cor}(r_s, \xi)$ are shown in figure 3 as a function of ξ^2 for $r_s = 1$ and $R_0 = a^*$. We note that $\varepsilon_{cor}(r_s, \xi)$ is nearly proportional to ξ^2. However, the slopes obtained within the STLS approach and the MSA approach are different. As we shall see in the following, this fact has considerable consequences for the spin-susceptibility obtained within the two approaches. We stress that we use a coupling-constant integration in order to calculate the ground-state energy.

4. Results

4.1. Spin susceptibility

A small magnetic field must be applied parallel to the wire axis and the magnetization must be measured in order to determine the spin-susceptibility. The spin-susceptibility of the free electron gas is given by $\kappa_0 = 16 r_s^3 a^*/\pi^2 \mathrm{Ry}^*$. For the interacting electron gas the spin-susceptibility κ_s, including exchange and correlation, is expressed as

$$\frac{\kappa_0}{\kappa_s} = 1 + \frac{8r_s^2}{\pi^2 \mathrm{Ry}^*} \left. \frac{\partial^2(\varepsilon_{ex} + \varepsilon_{cor})}{\partial \xi^2} \right|_{\xi \to 0} = 1 + \frac{\kappa_0}{\kappa_{s,ex}} + \frac{8r_s^2}{\pi^2} \alpha_s. \tag{6}$$

$\alpha_s = (1/\mathrm{Ry}^*)\partial^2 \varepsilon_{cor}(r_s, \xi)/\partial \xi^2|_{\xi \to 0}$ is called the spin-stiffness [5]. κ_s defines the static magnetic susceptibility X_M by

$$X_M = \mu_B^2 N^2 \kappa_s \tag{7}$$

and μ_B is the Bohr magneton. From the ground-state energy as function of the spin-polarization we can calculate the spin-susceptibility.

We obtain $\varepsilon_{ex}(r_s, \xi \to 0) = \varepsilon_{ex}(r_s, \xi = 0) - \xi^2 f(2k_F R_0)\mathrm{Ry}^*/8r_s$ [2] and $\kappa_{s,ex}$ can be calculated analytically: $\kappa_0/\kappa_{s,ex} = -2r_s f(2k_F R_0)/\pi^2$. We conclude that within the HFA the spin-susceptibility is given by [2]

$$\kappa_0/\kappa_{s,HFA} = 1 - 2r_s f(2k_F R_0)/\pi^2. \tag{8}$$

An instability point $\kappa_0/\kappa_{s,HFA} = 0$ occurs at $r_s = r_{scs,HFA}$ and $\kappa_0/\kappa_{s,HFA}$ becomes negative at low density $r_s > r_{scs,HFA}$. Such a behaviour is also found for the three-dimensional

electron gas [5]. Within the MSA the spin-susceptibility can be calculated analytically and is given by [2]

$$\kappa_0/\kappa_{s,MSA} = 1/[1 + 4r_s f(2k_F R_0)/\pi^2]^{1/2}. \tag{9}$$

We repeat that the MSA corresponds to the RPA and we note that $\kappa_0/\kappa_{s,MSA}$ is always positive.

A simple proposal to calculate the spin-susceptibility was given by Vosko, Wilk and Nusair (VWN) [9] for the three-dimensional electron gas. Accordingly, α_s is given by

$$\alpha_{s,VWN} = \alpha_{s,MSA}\frac{\varepsilon_{cor}(r_s, \xi = 1) - \varepsilon_{cor}(r_s, \xi = 0)}{\varepsilon_{cor,MSA}(r_s, \xi = 1) - \varepsilon_{cor,MSA}(r_s, \xi = 0)}. \tag{10}$$

$\alpha_{s,MSA}$ is given in terms of the interaction potential as [2]

$$\alpha_{s,MSA} = -\frac{\pi^2}{8r_s^2}\left[1 - \frac{1}{[1 + 4r_s f(2k_F R_0)/\pi^2]^{1/2}} - \frac{2}{\pi^2}r_s f(2k_F R_0)\right]. \tag{11}$$

Within the VWN approach one only needs to know $\varepsilon_{cor}(r_s, \xi = 1)$ and $\varepsilon_{cor}(r_s, \xi = 0)$ within the STLS approach and the MSA. We believe that the VWN approach represents an interesting test of the spin-stiffness obtained from the correlation energy $\varepsilon_{cor}(r_s, \xi \to 0)$ within the ξ-dependent STLS approach. This test is useful because the polarization dependence of the ground-state energy is difficult to obtain within Monte Carlo calculations [10]. Within the STLS approach we numerically calculate α_s by

$$\alpha_s = 2[\varepsilon_{cor}(r_s, \xi_1) - \varepsilon_{cor}(r_s, \xi = 0)]/[\mathrm{Ry}^* \xi_1^2]. \tag{12}$$

We have chosen $\xi_1 = 0.3$ in our calculation and we have checked that with $\xi_1 = 0.2$ and $\xi_1 = 0.1$ we obtain nearly identical results.

The spin-stiffness α_s is shown in figure 4 versus r_s for $R_0 = a^*$. We note a difference between the STLS approach and the MSA: $\alpha_{s,MSA} > \alpha_s$. This becomes clear from figure 3. From a theoretical point of view figure 4 is the most important figure of the present paper. For large r_s we conclude from equation (6) that α_s must be calculated with high precision: the correlation contribution to the spin-susceptibility enter the calculation via $r_s^2\alpha_s$. In the future one should try to get more accurate values for the spin-stiffness, for instance by Monte Carlo calculations.

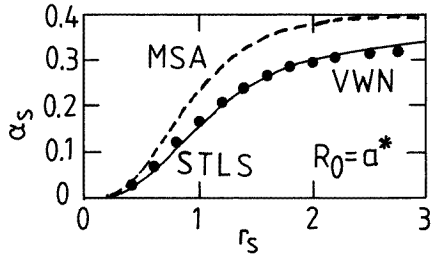

Figure 4. Spin-stiffness α_s versus Wigner–Seitz parameter r_s for $R_0 = a^*$ in different approximations. The solid and dashed lines represent the STLS approach and the MSA, respectively. The solid dots represent the VWN approach.

In figure 5 we show κ_0/κ_s versus r_s in various approximations for $R_0 = a^*$. Important is the fact that the STLS and the VWN approaches give similar results. Correlation effects give a positive contribution to the inverse spin-susceptibility, while exchange effects give a negative contribution. Moreover, the validity range of the HFA and the MSA is small: $r_s < 0.5 \approx 2r_s^*$ for $R_0 = a^*$. These results show that (i) correlation effects are important, compare with the HFA and (ii) correlation effects must be described using an LFC, compare with the MSA. We find a Bloch instability ($\kappa_0/\kappa_s < 0$) for $r_s > r_{scs} \approx 2r_{scs,HFA}$ [11] within

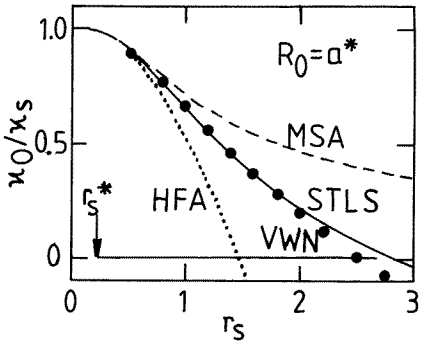

Figure 5. Inverse spin-susceptibility $1/\kappa_s$ (in units of the inverse spin-susceptibility of the free electron gas $1/\kappa_0$) versus Wigner–Seitz parameter r_s for $R_0 = a^*$ in different approximations. The solid, dashed and dotted lines represent the STLS approach, the MSA and the HFA, respectively. The solid dots represent the VWN approach. r_s^* for the application of the one-subband model is indicated.

Table 1. Inverse spin-susceptibility $1/\kappa_s$ (in units of the inverse spin-susceptibility of the free electron gas $1/\kappa_0$) for various values of r_s and the wire width parameter R_0 within the STLS approach. In the last lines we give values of r_s^* and r_{sce}.

	κ_0/κ_s				
r_s	$R_0 = a^*/5$	$R_0 = a^*/2$	$R_0 = a^*$	$R_0 = 2a^*$	$R_0 = 4a^*$
0.1	0.981	0.996	0.999	1.000	1.000
0.2	0.913	0.972	0.991	0.998	1.000
0.4	0.727	0.870	0.946	0.983	0.999
0.6	0.548	0.733	0.865	0.949	0.985
0.8	0.393	0.596	0.763	0.897	0.966
1.0	0.262	0.470	0.657	0.830	0.939
1.2	0.150	0.358	0.553	0.755	0.902
1.5	0.010	0.214	0.410	0.636	0.834
1.8	−0.102	0.095	0.277	0.520	0.755
2.0		0.008	0.216	0.448	0.699
2.5		−0.104	0.071	0.290	0.556
3.0			−0.034	0.166	0.424
3.5				0.074	0.309
4.0				0.013	0.217
4.5				−0.021	0.148
5.0					0.101
5.5					0.077
6.0					0.074
6.5					0.092
r_s^*	0.05	0.125	0.25	0.5	1.0
r_{sce}	1.02	1.43	1.95	2.56	3.63

the STLS and the VWN approximations, while this instability is absent within the MSA. The Bloch instability will be discussed in section 5 in detail.

Our numerical results for the spin-susceptibility within the STLS approach are given in table 1 for different values of R_0/a^* and r_s. We note that with increasing r_s and decreasing R_0 the ratio κ_0/κ_s decreases. The decrease of κ_0/κ_s is due to many-body effects (exchange and correlation).

From figure 5 we derive the relation $1/\kappa_{s,HFA} < 1/\kappa_s < 1/\kappa_{s,MSA}$. This motivated us to use an analytical expression $\kappa_{s,A}$ for the spin-susceptibility given by

$$\frac{\kappa_0}{\kappa_{s,A}} = \frac{1}{2}\left[(1-p)\frac{\kappa_0}{\kappa_{s,HFA}} + (1+p)\frac{\kappa_0}{\kappa_{s,MSA}}\right]. \tag{13}$$

A nice fit of our data in table 1 is obtained with (13) for $p = 0.55$, see figure 6. We note that $\kappa_0/\kappa_{s,A}$ has a large validity range ($r_s \leqslant 1.5 r_{scs,HFA}$) and holds for all values of R_0/a^* and can be used to fit experimental results by using R_0 as the fit parameter (assuming that the density is known). We believe that equation (13) is useful for experimenters.

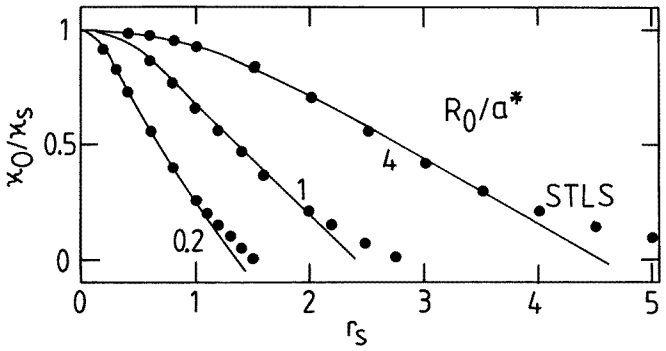

Figure 6. Inverse spin-susceptibility $1/\kappa_s$ (in units of the inverse spin-susceptibility of the free electron gas $1/\kappa_0$) versus Wigner–Seitz parameter r_s for $R_0 = a^*/5$, $R_0 = a^*$, and $R_0 = 4a^*$ within the STLS approach as the solid dots. The solid lines represent (13) with $p = 0.55$.

4.2. Collective excitations

The charge-density and the spin-density response functions are determined by effective interaction potentials. For small wavenumbers these effective interaction potentials are determined by sum rules for the compressibility κ_c and the spin-susceptibility κ_s [12]. The compressibility of the quasi-one-dimensional electron gas with cylindrical confinement was calculated in [7]. The application of the sum-rules to quantum wires [13] leads to the following equations for the long-wavelength collective charge-density modes $\omega_c(q \to 0)$ and spin-density modes $\omega_s(q \to 0)$:

$$\omega_c(q \to 0) = v_F|q|[4r_s f(qR_0 \to 0)/\pi^2 + \kappa_0/\kappa_c]^{1/2} \tag{14a}$$

and

$$\omega_s(q \to 0) = v_F|q|[\kappa_0/\kappa_s]^{1/2}. \tag{14b}$$

$v_F = k_F/m^*$ is the Fermi velocity. Since $f(x \ll 1) = 4\ln(2/x)$, in the long-wavelength limit the charge-density excitations are only weakly modified by many-body effects contained in κ_0/κ_c, see (14*a*). (14*b*) shows that the spin-susceptibility determines the sound velocity v_s of the spin-density excitations defined by $\omega_s(q \to 0) = v_s|q|$. We obtain $v_s = v_F[\kappa_0/\kappa_s]^{1/2} < v_F$ and many-body effects are essential to predict the spin-sound velocity.

In figure 7 we show $\omega_c(q \to 0)/v_F|q|$ for $qa^* = 0.1$ and $\omega_s(q \to 0)/v_F|q|$ versus r_s for different wire radii. We note that the spin-density modes are below and the charge-density modes are above the electron–hole (eh) excitation spectrum given by $\omega_{eh}(q \to 0) = v_F|q|$. Similar results have been obtained before for $\omega_c(q)$ [1, 6, 7, 13]. However, our results shown in figure 5 demonstrate that the HFA is not a quantitative theory to describe spin-density excitations. Spin-density excitations within the HFA have been discussed recently [14]. We conclude from our results shown in figure 5 that correlation effects are very important

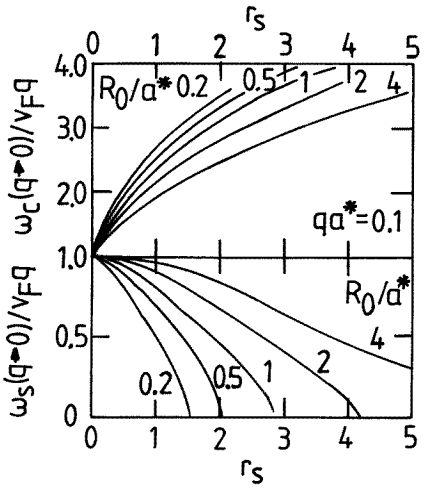

Figure 7. Charge-density excitations $\omega_c(q \to 0)/v_F q$ and spin-density excitations $\omega_s(q \to 0)/v_F q$ versus Wigner–Seitz parameter r_s according to (14) for different confinement parameters R_0. $\omega_c(q \to 0)/v_F q$ is calculated for $qa^* = 0.1$. Our results contain exchange and correlation effects. Note the different scales for $\omega_c(q \to 0)$ and $\omega_s(q \to 0)$.

for a quantitative analysis of v_s [2]. Exchange-only calculations [14] overestimate many-body effects for spin-density excitations and cannot be trusted. Compared to the HFA, the prediction of the STLS approach are quite spectacular: for $r_s = r_{scs,HFA}$ we derive $\kappa_0/\kappa_{s,HFA} = 0$ and $\omega_{s,HFA}(q \to 0)/v_F|q| = 0$ within the HFA, while we find $\kappa_0/\kappa_s \approx 0.4$ and $\omega_s(q \to 0)/v_F|q| \approx 0.63$ within the STLS approach.

Collective modes in quantum wires have also been calculated within the bosonization approach [15]. In this approach one neglects electron–hole excitations. We note that the existence of electron–hole excitations has been shown by experiment. The collective modes in the bosonization approach [15] are described by unspecified functions. As long as these functions are not specified it seems that the predictive power of this theory approaches zero.

5. Discussion

5.1. Validity range and the Bloch instability

In the present paper we studied a cylindrical confinement model for quantum wires where the interaction potential is given in analytical form [6]. We used in our calculation a one-subband model and the Fermi energy must be smaller than the intersubband energy (between the first and the second subband). One obtains the condition $r_s > r_s^* \approx 0.25 R_0/a^*$. From our numerical results we found a Bloch instability [11] at a critical (c) Wigner–Seitz parameter r_{sc}. Some values for r_{sc}, as found from the ground-state energy condition $\varepsilon_0(r_{sce}, \xi = 0) = \varepsilon_0(r_{sce}, \xi = 1)$ (r_{sce} with e for energy) or from the spin-susceptibility condition $\kappa_0/\kappa_s(r_{scs}) = 0$ (r_{scs} with s for susceptibility), are given in table 2. The simplest estimate of the validity range of our results is to argue that for $r_s^* < r_s < r_{sce}$ our results should be valid, supposing that the STLS approach gives accurate results for the ground-state energy and for κ_s.

The validity range of the STLS approach is difficult to estimate. From a similar calculation for the three-dimensional electron gas and a comparison with quasi-exact Monte Carlo calculations [16] we estimate the validity range of the *spin-susceptibility* calculations within the STLS-approach as $r_s < 2r_{scs,HFA}$ ($r_{sce,HFA} \approx r_{scs,HFA}$) [17]. A similar conclusion is obtained by applying our method to a one-dimensional electron gas with short-range interaction and comparing with quasi-exact results [18]: for $r_s/r_{scs,HFA} < 1$

Table 2. Instability point r_{sc} for the Bloch instability for various values of the width parameter R_0. In the first three columns we show the value r_{sce} (with e for energy and defined by $\varepsilon_0(r_{sce}, \xi = 0) = \varepsilon_0(r_{sce}, \xi = 1)$), calculated within the HFA ($r_{sce,HFA}$) and the STLS approach (r_{sce}). In the last three columns we show the value r_{scs} (with s for susceptibility and defined by $\kappa_0/\kappa_s = 0$) within the HFA ($r_{scs,HFA}$) and the STLS approach (r_{scs}).

R_0/a^*	$r_{sce,HFA}$	r_{sce}	$r_{sce}/r_{sce,HFA}$	$r_{scs,HFA}$	r_{scs}	$r_{scs}/r_{scs,HFA}$
0.2	0.72	1.02	1.4	0.75	1.52	2.0
0.5	1.01	1.43	1.4	1.08	2.04	2.0
1.0	1.36	1.95	1.4	1.46	2.85	2.0
2.0	1.88	2.56	1.4	2.06	4.17	2.0
3.0	2.30	3.11	1.4	2.55	5.4	2.1
4.0	2.66	3.63	1.4	2.98	≈ 6	≈ 2

our approach is quantitatively correct, while for $1.5 < r_s/r_{scs,HFA} < 2$ an error smaller than 10% could appear. For the present model and for $R_0/a^* = 1$ this means that our results for κ_s should be valid for $0.25 < r_s < 2r_{scs,HFA} = 2.9$. Note that for $R_0/a^* = 1$ we found $r_{sce} = 1.95$ and $r_{scs} = 2.85$. This shows that concerning the existence of the Bloch instability we cannot make a definitive statement because our theory is not exact.

According to the results obtained in [17] and [18] our numerical results for the spin-susceptibility and the spin-density excitations can be trusted for

$$r_s^* < r_s < 1.5r_{sce,HFA} \approx r_{sce}. \tag{15}$$

(15) represents a conservative estimate. For $r_s > 1.5r_{sce,HFA}$ we expect that our results are only qualitatively correct. We add that the HFA and the MSA have a very limited validity range $r_s^* < r_s < 2r_s^*$.

It was pointed out by Bloch that a three-dimensional electron gas becomes spin polarized at low electron density for $r_s > r_{sce,HFA} = 5.45$ [11]. This argument was given within the HFA. Correlation effects, obtained with Monte Carlo calculations, shift the instability point to $r_{sce} \approx r_{scs} \approx 70$ [16]. We conclude that in the three-dimensional electron gas $r_{sce}/r_{sce,HFA} \approx 13$ and the instability point is determined by correlation effects. For quasi-one-dimensional systems with a cylindrical confinement we found that a Bloch instability occurs within the STLS approach at relatively high density depending on the wire width R_0 [19]: $r_{sce}/r_{sce,HFA} \approx 1.4$ and correlation effects [20] are less important for the instability than exchange effects. Strictly speaking, the Bloch instability occurs at r_{sce} where $\varepsilon_0(r_{sce}, \xi = 0) = \varepsilon_0(r_{sce}, \xi = 1)$. We find that κ_s is finite at the density of the Bloch instability $r_{sce} \approx 1.4r_{sce,HFA}$. For $r_s < r_{sce}$ we found $\varepsilon_0(r_s, \xi = 0) < \varepsilon_0(r_s, \xi = 1)$ and for $r_s > r_{sce}$ we obtained $\varepsilon_0(r_s, \xi = 1) < \varepsilon_0(r_s, \xi = 0)$. If we define r_{scs} as the critical Wigner–Seitz parameter where $\kappa_0/\kappa_s = 0$, another definition of the Bloch instability, we obtain numerically the relation $r_{scs} \approx 2r_{scs,HFA}$ with $r_{sce,HFA} \approx r_{scs,HFA}$, see table 2.

For a two-dimensional parabolic confinement in the xy-plane [21], with a wire width characterized by the length b, the critical Wigner–Seitz parameter was reported in [2] and for an anisotropic confinement model (with a one-dimensional parabolic confinement of width δ in the x-direction and a one-dimensional delta-confinement in the y-direction) [22] the critical density for the Bloch instability also was calculated [23]. In figure 8 we show the critical Wigner–Seitz parameter r_{sce} for the different models as a function of the wire width parameters R_0, b and δ. r_{sce} for the two-dimensional parabolic confinement is nearly a factor of two larger than for the cylindrical confinement. We note that for the parabolic confinement one also finds $r_{sce} \approx 1.4r_{sce,HFA}$ and the larger r_{sce} compared to the cylinder

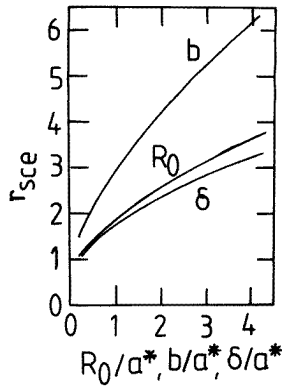

Figure 8. Critical Wigner–Seitz parameter r_{sce} versus width parameters R_0/a^*, b/a^* and δ/a^* for a cylindrical [19], a parabolic [2] and an anisotropic [23] confinement potential, respectively.

confinement is due to the softer potential for given r_s and $b = R_0$. We cannot give a definitive conclusion about the existence of the Bloch instability. As we argued in the last subsection a conservative estimate of the validity range of our calculation of the spin-susceptibility within the STLS approach is about $r_s^* \leqslant r_s \leqslant r_{sce}$.

It was predicted by Lieb and Mattis that the ground state of an interacting electron gas in one dimension is unmagnetized [24]. We cannot make predictions about the magnetization for $r_s > r_{sce}$: our ground-state energy calculation only suggests that for $r_s > r_{sce}$ the spin-degeneracy is lifted (the Fermi wavenumber k_F is multiplied by 2). Some arguments why the Lieb–Mattis theorem should not apply to the present model were discussed in [2]. We refer the reader to this reference and to our discussion of experiments.

5.2. Comparison with experiments

Recent experimental results [25–27] on ballistic transport in quantum point contacts seem to confirm the existence of a Bloch instability. A detailed analysis of the experiment performed in [26] has been given in [2]. Even if the Bloch instability does not exist (supposing that the Bloch instability is an artifact of our approximate theory) it is clear from our calculation that at $r_s > r_{sce}$ the ground-state energies of the unpolarized and the polarized one-dimensional interacting electron gas are nearly equal and a small magnetic field will polarize the electron gas. In fact, a finite magnetic field, applied parallel to the wire axis, gave experimental evidence for the existence of the Bloch instability [25–27].

In this paper we gave quantitative predictions for spin-density excitations in quantum wires. We showed that the spin-susceptibility determines collective spin-density excitations. Electronic Raman spectroscopy, as already performed [28–30], confirmed the existence of charge-density and spin-density waves together with particle–hole excitations. However, the experiments have been made at high electron densities and large wire radii where $\omega_s(q \to 0) \approx v_F|q|$. Many-body effects in this parameter range are small and a comparison with our theory is not conclusive: $v_s - v_F$ is very small and difficult to extract from the experimental results.

5.3. Electronic confinement models

We would like to suggest an experiment in order to obtain information about the quantum confinement for wires. Suppose that experimentally the collective modes (density and spin) and the electron–hole (eh) excitations of a quantum wire have been measured for

a given wavenumber q. The electron density can be determined from the one-particle excitations: $v_F = \omega_{eh}(q \to 0)/|q|$. The spin-density excitations can be used to obtain the width parameter (see equation (13) and equation (14*b*)), for instance within the cylindrical confinement. Then, the energy of the collective charge-density excitations is defined, for a given confinement model and a given wavenumber. If the theoretical prediction does not agree with the experimental value one has to modify the confinement model. Within a systematic study, one can obtain information about the electronic confinement potential in quantum wires. This could help to understand and improve technological processes used to fabricate quantum wires.

The confinement potential is an input function in our theory. Therefore, the 'real numbers' for the excitation spectrum within different confinement potentials must be known in order to give the experimenter a sufficient number of models ('options') to compare with experimental results. The cylindrical confinement, studied in the present paper, is in competition with the two-dimensional oscillator confinement potential [2, 21] and the anisotropic confinement [22, 23] potential studied before.

6. Conclusion

For a *cylindrical confinement model* we calculated the spin-susceptibility of the quasi-one-dimensional electron gas. Analytical and numerical results for the spin-susceptibility have been presented including exchange and correlation.

The excitation spectrum, consisting in charge-density waves, spin-density waves *and* electron–hole excitations, has been calculated in the long-wavelength limit. The validity range of our calculations has been discussed. Our theory for the collective modes is predictive and can be tested by Raman scattering experiments.

References

[1] Calmels L and Gold A 1997 *Phys. Rev.* B **56** 1762
[2] Calmels L and Gold A 1997 *Europhys. Lett.* **39** 539
[3] Singwi K S, Tosi M P, Land R H and Sjölander A 1968 *Phys. Rev.* **176** 589
[4] Singwi K S and Tosi M P 1981 *Solid State Physics* vol 36 (New York: Academic) p 177
[5] Pines D and Nozières P 1966 *The Theory of Quantum Liquids* vol 1 (New York: Benjamin)
[6] Gold A and Ghazali A 1990 *Phys. Rev.* B **41** 7626
[7] Calmels L and Gold A 1996 *Phys. Rev.* B **53** 10 846
[8] Zabolitzky J G 1980 *Phys. Rev.* B **22** 2353
[9] Vosko H, Wilk L and Nusair M 1980 *Can. J. Phys.* **58** 1200
[10] Perdew J P and Wang Y 1992 *Phys. Rev.* B **45** 13 244
[11] Bloch F 1929 *Z. Phys.* **57** 545
See Ashcroft N W and Mermin N D 1976 *Solid State Physics* (New York: Holt, Rinehart and Winston) ch 32
[12] Iwamoto N, Krotscheck E and Pines D 1984 *Phys. Rev.* B **29** 3936
[13] Gold A and Calmels L 1998 *Modulated Semiconductor Structures (MSS) VII (Santa Barbara, July 1997) Physica* E **2** at press
Gold A and Calmels L 1998 unpublished
[14] Brataas A, Mal'shukov A G, Gudmundsson V and Chao K A 1996 *J. Phys.: Condens. Matter* **8** L325
[15] Schulz H J 1993 *Phys. Rev. Lett.* **71** 1864
See also Sassetti M and Kramer B 1998 *Phys. Rev. Lett.* **80** 1485
[16] Ceperly D M and Alder B J 1980 *Phys. Rev. Lett.* **45** 566
[17] Gold A 1998 in preparation
[18] Gold A 1998 *J. Phys.: Condens. Matter* **10** 3547
Gold A 1998 *J. Phys.: Condens. Matter* **10** 3959
[19] Gold A and Calmels L 1996 *Phil. Mag. Lett.* **74** 33
[20] Gold A and Ghazali A 1990 *Phys. Rev.* B **41** 8318

[21] Friesen W I and Bergersen B 1980 *J. Phys. C: Solid State Phys.* **13** 6627
[22] Hu G Y and O'Connell R F 1990 *Phys. Rev.* B **42** 1290
[23] Gold A and Calmels L 1996 *Solid State Commun.* **100** 137
Calmels L and Gold A 1998 *Solid State Commun.* **106** 139
[24] Lieb E and Mattis D 1962 *Phys. Rev.* **125** 164
[25] Tscheuschner R D and Wieck A D 1996 *Superlatt. Microstruct.* **20** 615
[26] Thomas K J, Niccolls J T, Simmons M Y, Pepper M, Mace D R and Ritchie D A 1996 *Phys. Rev. Lett.* **77** 135
[27] Ramvall P, Carlsson N, Maximov I, Omling P, Samuelson L, Seifert W and Wang Q 1997 *Appl. Phys. Lett.* **71** 918
[28] Goñi A R, Pinczuk A, Weiner S J, Calleja J M, Dennis B S, Pfeiffer L N and West K W 1991 *Phys. Rev. Lett.* **67** 3298
[29] Schmeller A, Goñi A R, Pinczuk A, Weiner S J, Calleja J M, Dennis B S, Pfeiffer L N and West K W 1994 *Phys. Rev.* B **49** 14 778
[30] Schüller C, Biese G, Keller K, Steinebach C, Heitmann D, Grambow P and Eberl K 1996 *Phys. Rev.* B **54** R17 304